

**Informal Documentation**

**Characterization of the Neutron Spectrum  
in the UMass-Lowell Research Reactor**

**Dr. John R. White  
Chemical and Nuclear Engineering Department  
University of Massachusetts Lowell**

**January 9, 1998**

# Characterization of the Neutron Spectrum in the UMass-Lowell Research Reactor

Dr. John R. White  
Chemical and Nuclear Engineering Department  
University of Massachusetts Lowell  
January 9, 1998

## Introduction

This work involves the development and analysis of some 2-D analytical models for the characterization of the neutron flux spectra in the UMass-Lowell Research Reactor (UMLRR). In-depth knowledge of the neutron spectra in the radiation basket locations is needed to plan and analyze irradiation experiments performed in the baskets. Of particular interest in many materials studies is the neutron spectrum in the high energy regions (above 0.1 MeV) in the primary radiation basket assemblies where the bulk of the material characterization and irradiation experiments are made.

This work is a continuation of a brief study performed during Summer 1997. The Phase I effort utilized a relatively simple 1-D model of the UMLRR to obtain preliminary estimates of the spectrum in the basket locations. In the current Phase II effort, a set of 2-D XY computational models of the current HEU core and basket arrangement have been developed and more accurate estimates of the neutron and gamma spectra within the radiation basket assemblies have been determined. The 2-D calculations used both VENTURE<sup>1</sup> diffusion theory and DORT<sup>2</sup> transport theory models. The primary goal of the few-group VENTURE calculations was to determine the power distribution within the core, which was then used to develop a distributed source for the multigroup DORT fixed source computation. The DORT model used a coupled neutron-gamma library of multigroup cross sections, with 47 neutron groups and 20 gamma groups. This fairly detailed representation of the energy domain gives good resolution across the full energy range of interest, including about 25 neutron energy groups above 0.1 MeV.

This report summarizes the work performed as part of this study. In particular, it highlights the cross section development, overviews the 2-D models used to develop the estimates of the flux spectra in the UMLRR, and it discusses the results of the 2-D analyses. The focus here is on the spatial and spectral distribution of the neutron and gamma fluxes in the vicinity of the baskets, and on several integral spectral indices that characterize the overall spectrum (i.e. some broad group fluxes). An effort is also made to fully discuss and document the base models developed here, since it is expected that these will serve as the basis for future work in this area.

## Computational Procedure for the Cross Sections

Generating effective group constants for performing reactor physics computations is a complicated process. Since most 1-D and 2-D core and shielding calculations use the multigroup approximation and they use homogenized regions to describe the real geometric configuration of interest, the 'effective' nuclear data used in such calculations must account for both the fine group resonance effects and the real heterogeneous geometry of the system. This is achieved by performing *resonance calculations* to treat the spectral self shielding and by performing

*assembly or cell calculations* to account for spatial self shielding. In the present work, these computations are accomplished with the BONAMI and XSDRN modules of the SCALE 4.3 system.<sup>3</sup> Other modules (such as AJAX, NITAWL, WAX, etc.) were also used to select appropriate isotopes from the main ENDF/B-VI VITAMIN-B6 199/42 group coupled library,<sup>4</sup> convert the cross section format to a form compatible with the different codes, and to merge individual isotopes into a final library for use in subsequent 1-D and 2-D core calculations.

The specific computations for the UMLRR required a set of the three calculations - one each for the full fuel assembly, partial assembly, and control blade. These sequences treated the resonance self shielding for the specific isotope densities present for these systems, and they approximated the spatial self shielding with a detailed plate-by-plate heterogeneous 1-D model of a unit assembly. The resultant effective cross sections were then combined with data from an infinite medium homogeneous model for the materials outside the core (water, aluminum, graphite, etc.) to give a library suitable for 1-D or 2-D homogeneous full core analyses.

Up to this point the cross sections still have the original fine-group representation (199 neutron groups and 42 gamma groups). This level of energy detail is suitable for 1-D core calculations, but it has too much fine structure for reasonable 2-D computational times (even with today's fast computers). Thus, a final step, using a generic 1-D model of the reactor, was performed to determine a typical fine-group weighting function and to collapse the fine-group library to a broad-group set for subsequent 2-D calculations. This step was performed twice - once to give a 2-group library for simple diffusion theory calculations (used for computing  $k_{\text{eff}}$  and power distributions) and a second time to create a 47/20 group coupled library for transport theory analyses (typically used to determine neutron and gamma spectra in 2-D configurations using a fixed source determined from a diffusion theory run).

In summary, this work generated three nuclear data libraries that can be utilized in subsequent UMLRR core analyses, as follows:

- UMLRRXSD.LIB - 199/42 group library for use with 1-D XSDRN core models<sup>3</sup>
- UMLRR2G.BCD - 2 group data in ANISN format for VENTURE models<sup>1</sup>
- UMLRR67G.BCD - 47/20 group data in ANISN format for DORT calculations<sup>2</sup>

The UMLRRXSD.LIB dataset was utilized in the Phase I study to estimate the neutron and gamma spectra in the radiation basket locations in the UMLRR. This study used a simple 1-D XSDRN model of the current core configuration (with fresh fuel). The other two libraries were used in the Phase II 2-D spectral studies for the UMLRR. Preliminary versions of the two broad-group libraries were generated as part of the Phase I effort, but these were updated in the current project using a new approach for obtaining broad group data (see below).

### **The 1-D UMLRR HEU XSDRN Models**

There were four XSDRN models used in the generation of the three libraries summarized above. The first three configurations represent "assembly models" that try to account for the detailed heterogeneity that actually occurs within the full and partial fuel assemblies and in the control blade cell. These models were put together many years ago (close to 10 years now) and they have not changed significantly since that time. There was never any formal documentation but there are some informal notes available that gives a good overview of the basic setup for these specific component models.

The purpose of this section is to be a little more formal about the documentation of the fourth model in the sequence - that is the 1-D full core configuration used to determine a weight function for the energy collapse of the cross sections to some broad group structure (2 groups and 47/20 groups in this work). This 1-D XSDRN model represents a slice through the reactor core in the direction parallel to the two rows of control blades (thus the control blades never enter into the model). Control material is incorporated in the model by a rough 1-D simulation of the regulating rod.

The actual 1-D geometry with corresponding zone dimensions and descriptions is given in Table 1 and the material concentrations used are in Table 2. These data are consistent with the reference operating configuration for the UMLRR with fresh 93 w/o fuel loaded into the core (Core L). The 93 w/o fuel is referred to as high enriched uranium (HEU) fuel. Notice that each grid location (except the regulating rod location) contains a single homogenized zone containing either a radiation basket (RB), graphite reflector (GR), partial HEU fuel assembly (PA), or full HEU fuel assembly (FA). The partial element in the UMLRR has the same macroscopic geometry as the full fuel assembly, except that it only has half the  $^{235}\text{U}$  loading in each fuel plate (the fuel meat thickness is one-half that of the full fuel plate and the cladding thickness is modified accordingly so as to keep the same plate thickness). The regulating rod position is broken into three regions - a control zone that contains a homogenized mix of boral sandwiched between aluminum clad, and a zone which surrounds the control material containing a mixture of aluminum and water. This geometry should account for all the key features present in the real system and allow a reasonable weight function to be determined for collapsing the fine group data to some broad group level.

As indicated above, this model was run twice with the goal of generating a 2-group library and a coupled 47/20 group dataset for different end uses (one for VENTURE calculations and one for DORT analyses). Some final processing of these two libraries is necessary before they can be used directly - however, this final step is done within either the VENTURE or DORT systems as appropriate. For example, for VENTURE one must convert the ANISN formatted file into ISOTXS format and then into GRUPXS format before actual use. For DORT, one uses the GIP code to put the cross sections into group-ordered format for actual use in DORT (this code also does the cross section mixing to get macroscopic data).

Finally, one should note that the 1-D XSDRN model used here, although only slightly different from the one used in the Phase I study, represents a fundamental change in philosophy. Difficulty with the diffusion coefficients from the Phase I library development prompted the new model and new approach adopted here. The key difference is that the energy collapse for all the isotopes is done with the 1-D core model, whereas the assembly calculations were used previously. This approach gives a more realistic estimate of the neutron currents in the system (the "assembly models" used reflected or zero-current boundary conditions). Since the diffusion coefficient is current weighted, the new approach generally gives better estimates for this quantity for all regions and all isotopes.

Validation of the new procedure for determining the broad-group cross sections was done with comparisons to UMLRR VENTURE calculations made several years ago.<sup>5</sup> Since good agreement was obtained and the procedure gives more consistent behavior of the transport cross section, this new approach will become the basis for any future data generation needs (for diffusion theory analyses).

Table 1. Geometry details for 1-D UMLRR XSDRN model used for the cross section collapse.

Zone Description	Zone Width (cm)	Total Distance (cm)	Zone #	Material # (Reference)	# of Mesh
water	40.0000	40.0000	1	1	20
water+core box	1.5875	41.5875	2	2	1
grid location #1	7.7724	49.3599	3	3	8
grid location #2	7.7724	57.1323	4	5	8
grid location #3	7.7724	64.9047	5	6	8
grid location #4	7.7724	72.6771	6	7	8
grid location #5	7.7724	80.4495	7	7	8
grid location #6	7.7724	88.2219	8	7	8
grid location #7	7.7724	95.9943	9	7	8
grid location #8	7.7724	103.7667	10	7	8
grid location #9a	3.4100	107.1767	11	4	4
grid location #9b	0.9524	108.1291	16	12	2
grid location #9c	3.4100	111.5391	11	4	4
core box+water+clad	1.5875	113.1266	12	8	1
lead shield	7.6200	120.7466	13	9	5
clad+water+clad	2.8575	123.6041	14	10	2
thermal column	60.0000	183.6041	15	11	20

Table 2. Material composition (atom/b-cm) for the 1-D XSDRN model described in Table 1.

Material	Matl ID	<sup>235</sup> U	<sup>238</sup> U	<sup>27</sup> Al	<sup>12</sup> C	<sup>16</sup> O	<sup>1</sup> H	<sup>10</sup> B	<sup>nat</sup> Cd	Pb**
Water Refl	1	—	—	—	—	3.343-2	6.686-2	—	—	—
Water+Core Box	2	—	—	2.410-2	—	2.006-2	4.012-2	—	—	—
Rad Basket+Air	3	—	—	1.366-2	—	2.066-2	4.133-2	—	1.000-12	—
Rad Basket+Water*	4	—	—	1.164-2	—	2.697-2	5.394-2	—	—	—
Graphite Refl	5	—	—	2.998-3	7.068-2	2.318-3	4.636-3	—	—	—
Partial Fuel	6	4.697-5	3.490-6	2.537-2	—	1.930-2	3.860-2	1.000-12	—	—
Full Fuel	7	9.393-5	6.981-6	2.527-2	—	1.930-2	3.860-2	1.000-12	—	—
Core Box+Water+Clad	8	—	—	3.614-2	—	1.337-2	2.674-2	—	—	—
Lead Shield	9	—	—	—	—	—	—	—	—	3.296-2
Clad+Water+Clad	10	—	—	4.686-2	—	7.428-3	1.486-2	—	—	—
Thermal Column	11	—	—	—	8.023-2	—	—	—	—	—
Boral+Clad	12	—	—	4.532-2	7.874-3	—	—	5.145-3	—	—

\* This homogeneous material models a water-filled radiation basket. The basket with an air-filled bayonet is modeled as Matl #3. In the current model, the regulating rod region (without control) is modeled as a radiation basket filled with water (i.e. Matl #4).

\*\* This density is the sum of the individual isotope densities comprising lead, where <sup>206</sup>Pb = 7.910-3, <sup>207</sup>Pb = 7.251-3, and <sup>208</sup>Pb = 1.780-2 atom/b-cm.

### Strategy for the 2-D Spectrum Calculations

Transport theory analyses are generally computationally intensive but, for fixed-source computations with no upscatter, only one outer iteration is required within the code solution algorithm. Since this represents a significant improvement in runtime relative to eigenvalue or fixed-source problems with upscatter (i.e. problems requiring multiple outer iterations), this mode of operation is definitely the preferred solution scheme. However, since the core physics problem is really an eigenvalue problem, the overall problem solution becomes at least a two-step process -- first we have to compute the fission source, and then this distributed source is used to drive a fixed source transport problem.

In equation form, we can represent the core physics problem as an eigenvalue problem of the form

$$(L - \lambda F)\phi = 0 \quad (1)$$

where  $L\phi$  accounts for the loss and scattering components of the particle balance equation and  $F\phi$  represents the fission source term. The eigenvalue,  $\lambda$ , is simply the inverse of the multiplication factor ( $\lambda = 1/k_{\text{eff}}$ ).

If the fission source term is moved to the right hand side of eqn. (1), then the balance equation can be written as

$$L\phi = \lambda F\phi = Q \quad (2)$$

For known  $Q$ , this expression becomes a fixed-source problem.

The VENTURE code is used to solve eqn. (1) using a few-group diffusion theory approximation. In the vicinity of the core, diffusion theory is quite adequate and it gives a good estimate of the eigenvalue and power distribution within the fueled regions. The neutron source distribution needed for use with eqn. (2) is simply related to the power distribution, as described below.

First let's denote  $PD(\vec{r})$  as the power density distribution, where

$$PD(\vec{r}) = \kappa \sum_g \Sigma_{fg'}(\vec{r}) \phi_{g'}(\vec{r}) \quad (3)$$

where the symbols have their traditional meaning and  $\kappa$  gives the average energy release per fission. Now, the multigroup fission source,  $Q_g(\vec{r})$ , is given by

$$Q_g(\vec{r}) = \lambda \chi_g \sum_{g'} \nu \Sigma_{fg'}(\vec{r}) \phi_{g'}(\vec{r}) \quad (4)$$

Combining eqns. (3) and (4) gives

$$Q_g(\vec{r}) = \alpha \chi_g PD(\vec{r}) \quad (5)$$

where the power-to-source conversion factor,  $\alpha$ , is given by

$$\alpha = \lambda \nu / \kappa \quad (6)$$

For an eigenvalue near unity,  $\nu \approx 2.43$  neutrons per fission, and  $\kappa \approx 200$  MeV per fission, the conversion factor becomes  $\alpha \approx 7.6 \times 10^{10}$  n's/cm<sup>3</sup> – s per watt/cm<sup>3</sup>.

Thus, the overall strategy for performing the spectral calculations in DORT involves a four-step process:

1. Perform VENTURE few-group diffusion theory calculations for the desired configuration to determine the power density distribution,  $PD(\vec{r})$ .
2. Using eqns. (5) and (6), generate the source density distribution,  $Q_g(\vec{r})$ , for use in DORT.
3. Perform DORT multigroup fixed-source transport calculations to determine the space and energy dependent flux distribution,  $\phi_g(\vec{r})$ , for the configuration of interest.
4. Process the large amount of data from DORT into useable form (i.e. determine fast, epithermal, and thermal fluxes for plotting purposes, perform reaction rate integrals as needed, etc.).

Several small Matlab and Fortran codes have been written to assist in the manipulations involved in Steps 2 and 4. Although not fully automated, once the VENTURE and DORT models have been developed, running through this sequence of four steps is relatively straightforward. The analyses leading up to the final results for this work (see later sections) follows this basic solution strategy.

### The 2-D HEU Configuration (Core L-1-1)

The UMass-Lowell Research Reactor (UMLRR) contains a 9x7 grid of fuel assemblies, graphite reflector elements, radiation baskets, and corner posts. It also has two grid locations reserved for an external neutron source and a low-worth regulating rod for fine reactivity control. Four large control blade assemblies are used for gross reactivity control and for flux shape adjustments. From the top view, the reactor is enclosed by an aluminum core box and a large pool of demineralized water surrounds the system on three sides, with a 3" lead shield and large graphite thermal column on the remaining side. A specific arrangement of fuel elements (both full and partial assemblies), graphite reflector blocks, and radiation baskets make up a particular core configuration. The current HEU core arrangement is denoted as Core L-1-1 and the basic layout for Core L-1-1 is pictured in Fig. 1.

Putting together a computational model for any reactor system requires precise information about the geometry and material composition of the actual system. It also requires a number of decisions by the model builder concerning the mesh grid layout, the zone placement, and the degree of detail that can be modeled efficiently and accurately within the limitations of the basic theory, the numerical methods used, and the capability of the available computer tools. These decisions often require that tradeoffs be made in the model detail, and these usually result in the consolidation of the fine heterogeneous geometry details into larger homogeneous regions. The homogeneous zones use properly averaged material densities to approximate the actual materials present in the real system.

In this work, each interior grid location within the UMLRR geometry (the central 7x5 grid array) was broken into a 5-region, 3-zone symmetric configuration, with two sides (top and

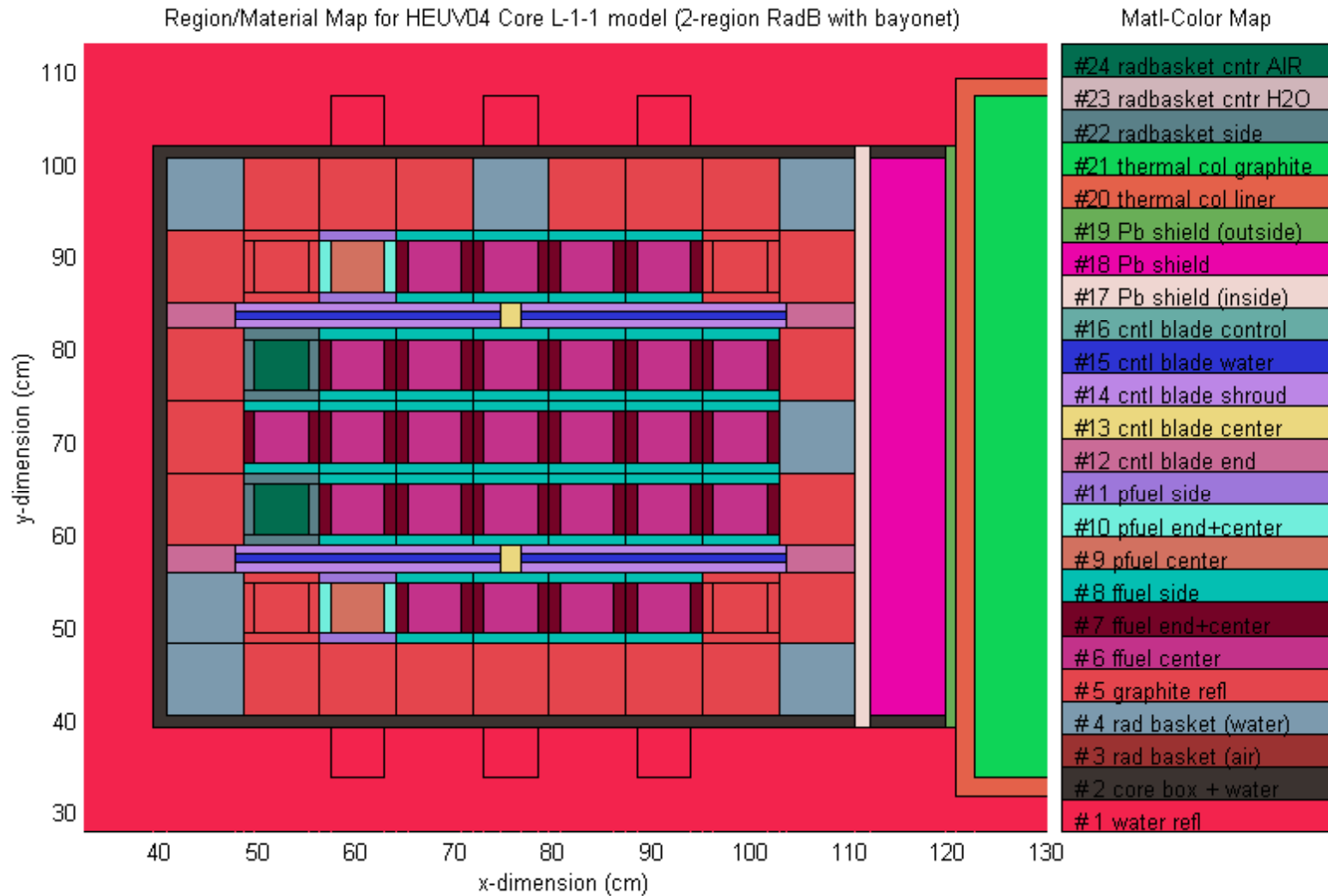


Fig. 1. Basic geometry and material layout for Core L-1-1.

bottom), two edges (left and right), and a center region. This zone layout and the specific dimensions used are consistent with the HEU fuel assembly geometry. This arrangement allows explicit modeling of the side plate and central fueled regions of the fuel assembly. It even allows for treatment of the slightly increased water content associated with the end plates and end water channel. This explicit 5-region, 3-zone model for each interior grid location is apparent in the Core L-1-1 configuration shown in Fig. 1. The remaining structures (control blades, corner posts, lead shield, thermal column, etc.) are also displayed explicitly in this diagram.

Getting the actual geometry and homogenized material information into the VENTURE and DORT codes requires specification of three key arrays: a fine mesh grid layout, a zone by mesh map, and a material by zone array. The details required for each of the codes are somewhat different, but the end result is identical. In particular, the zone or region boundaries with the desired mesh spacing for the UMLRR geometry are specified in Tables 3 and 4, respectively, for the x-direction and y-direction region boundaries. In the present model a 130x102 grid was chosen, spanning 200 cm in the x direction and nearly 142 cm in the y direction.

A zone by mesh map is then given which identifies a specific zone ID with each mesh point in the 2-D grid structure. For the current model, the zone numbers range from 1 to 176 (for ease in modeling, some zones numbers were not used). Attention to detail in specifying the zone and mesh map allows one to build a relatively flexible geometry that can handle a variety of material configurations. This modeling step is quite important, because a little added flexibility here can save lots of analysis time if several material layouts need to be considered.

The final zone by mesh map for the current calculation is given in Fig. 2. This map was extracted from the DORT output file, with a portion of the top, bottom, and right side truncated for ease of presentation. Careful review of this zone map shows that all the geometric details from Fig. 1 are included in the DORT computational model. The same zone configuration is modeled in VENTURE -- the notation is just a little different.

With a flexible geometry properly modeled, one now simply specifies a particular material composition to be placed in each zone (i.e. the so-called material by zone map). Homogenized atom densities for 24 materials were computed based on the nominal region densities and region volume fractions within the given homogeneous zone. The actual isotope densities for each of these homogeneous material zones are given in Table 5 and a slightly more descriptive identification is given in Table 6. Note that this latter description is inserted directly within some of the input files as internal documentation and for easy identification of the materials used. Note also that the fuel densities given in Table 5 for the HEU fuel zones are representative of fresh fuel (burnup information by assembly is not readily available).

For the Core L-1-1 configuration, the system has two partial HEU fuel assemblies, 27 full HEU fuel elements, two radiation baskets with air-filled bayonets inserted, etc. with the specific arrangement as shown in Fig. 1. This material layout was encoded into the material by zone array and the resultant material by mesh map is given in Fig. 3. Again, the data in this figure were extracted directly from the DORT output file, and careful review of the material layout verifies proper modeling of the desired Core L-1-1 configuration. With the mesh, zone, and material configurations specified and the material composition defined (see Figs. 1-3 and Tables 3-6), the model building process is complete. One is now ready to do the actual neutronics calculations in the VENTURE and DORT codes.

Table 3. X-direction region boundaries for the UMLRR 2-D XY geometry.

Primary Region Description	Secondary Region Description	Dimensions in cm		Dimensions in inches		# Mesh	Total Mesh
		Thickness	Total Dist.	Thickness	Total Dist.		
water reflector	water, water, everywhere	39.3650	39.3650	15.4980	15.4980	20	20
water refl + core box	water(0.5) + Al(0.5)	1.2700	40.6350	0.5000	15.9980	1	21
grid location #1	rad basket or graphite refl	6.9643	47.5993	2.7419	18.7399	7	28
7.7724	basket/refl & control shroud end	0.8081	48.4074	0.3181	19.0580	1	29
grid location #2	edge(0.4322) + center (0.5678)	1.1557	49.5631	0.4550	19.5130	1	30
7.7724	center	5.4610	55.0241	2.1500	21.6630	6	36
	edge(0.4322) + center (0.5678)	1.1557	56.1798	0.4550	22.1180	1	37
grid location #3	fuel edge(0.4322) + fuel center (0.5678)	1.1557	57.3355	0.4550	22.5730	1	38
7.7724	fuel center	5.4610	62.7965	2.1500	24.7230	6	44
	fuel edge(0.4322) + fuel center (0.5678)	1.1557	63.9522	0.4550	25.1780	1	45
grid location #4	fuel edge(0.4322) + fuel center (0.5678)	1.1557	65.1079	0.4550	25.6330	1	46
7.7724	fuel center	5.4610	70.5689	2.1500	27.7830	6	52
	fuel edge(0.4322) + fuel center (0.5678)	1.1557	71.7246	0.4550	28.2380	1	53
grid location #5	fuel edge(0.4322) + fuel center (0.5678)	1.1557	72.8803	0.4550	28.6930	1	54
7.7724	fuel center	1.7700	74.6503	0.6969	29.3899	2	56
	fuel center + control center structure	1.9210	76.5713	0.7563	30.1462	2	58
	fuel center	1.7700	78.3413	0.6969	30.8430	2	60
	fuel edge(0.4322) + fuel center (0.5678)	1.1557	79.4970	0.4550	31.2980	1	61
grid location #6	fuel edge(0.4322) + fuel center (0.5678)	1.1557	80.6527	0.4550	31.7530	1	62
7.7724	fuel center	5.4610	86.1137	2.1500	33.9030	6	68
	fuel edge(0.4322) + fuel center (0.5678)	1.1557	87.2694	0.4550	34.3580	1	69
grid location #7	fuel edge(0.4322) + fuel center (0.5678)	1.1557	88.4251	0.4550	34.8130	1	70
7.7724	fuel center	5.4610	93.8861	2.1500	36.9630	6	76
	fuel edge(0.4322) + fuel center (0.5678)	1.1557	95.0418	0.4550	37.4180	1	77
grid location #8 (no reg rod)	fuel edge(0.4322) + fuel center (0.5678)	1.1557	96.1975	0.4550	37.8730	1	78
7.7724	fuel center	5.4610	101.6585	2.1500	40.0230	6	84
	fuel edge(0.4322) + fuel center (0.5678)	1.1557	102.8142	0.4550	40.4780	1	85
grid location #9 (no reg rod)	basket/refl & control shroud end	0.8081	103.6223	0.3181	40.7962	1	86
7.7724	rad basket or graphite refl	6.9643	110.5866	2.7419	43.5380	7	93
core box+gap+shield clad	water(0.400) + Al(0.600)	1.5875	112.1741	0.6250	44.1630	1	94
lead shield	pure lead	7.6200	119.7941	3.0000	47.1630	4	98
shield clad + water gap	water(0.6666) + Al(0.3334)	0.9525	120.7466	0.3750	47.5380	1	99
thermal column clad	Al clad	1.9050	122.6516	0.7500	48.2880	1	100
thermal column	graphite, graphite, everywhere	77.3484	200.0000	30.4521	78.7402	30	130

Table 4. Y-direction region boundaries for the UMLRR 2-D XY geometry.

Primary Region Description	Secondary Region Description	Dimensions in cm		Dimensions in inches		# Mesh	Total Mesh
		Thickness	Total Dist.	Thickness	Total Dist.		
water reflector	water, water, everywhere	31.9950	31.9950	12.5965	12.5965	15	15
water refl or graphite refl clad	water or Al clad	1.9050	33.9000	0.7500	13.3465	1	16
water refl or thermal col	water or graphite	5.4650	39.3650	2.1516	15.4980	3	19
water refl + core box	water(0.5) + Al(0.5)	1.2700	40.6350	0.5000	15.9980	1	20
grid location A	rad basket or graphite refl	7.7724	48.4074	3.0600	19.0580	8	28
grid location B	side	1.1557	49.5631	0.4550	19.5130	1	29
	7.7724 center	5.4610	55.0241	2.1500	21.6630	6	35
	side	1.1557	56.1798	0.4550	22.1180	1	36
control location	control shroud	0.9716	57.1514	0.3825	22.5006	1	37
	2.8957 control center	0.9525	58.1039	0.3750	22.8756	1	38
	control shroud	0.9716	59.0755	0.3825	23.2581	1	39
grid location C	fuel side	1.1557	60.2312	0.4550	23.7131	1	40
	7.7724 fuel center	5.4610	65.6922	2.1500	25.8631	6	46
	fuel side	1.1557	66.8479	0.4550	26.3181	1	47
grid location D (no reg rod)	fuel side	1.1557	68.0036	0.4550	26.7731	1	48
	7.7724 fuel center	5.4610	73.4646	2.1500	28.9231	6	54
	fuel side	1.1557	74.6203	0.4550	29.3781	1	55
grid location E	fuel side	1.1557	75.7760	0.4550	29.8331	1	56
	7.7724 fuel center	5.4610	81.2370	2.1500	31.9831	6	62
	fuel side	1.1557	82.3927	0.4550	32.4381	1	63
control location	control shroud	0.9716	83.3643	0.3825	32.8206	1	64
	2.8957 control center	0.9525	84.3168	0.3750	33.1956	1	65
	control shroud	0.9716	85.2884	0.3825	33.5781	1	66
grid location F	fuel side	1.1557	86.4441	0.4550	34.0331	1	67
	7.7724 fuel center	5.4610	91.9051	2.1500	36.1831	6	73
	fuel side	1.1557	93.0608	0.4550	36.6381	1	74
grid location G	rad basket or graphite refl	7.7724	100.8332	3.0600	39.6981	8	82
water refl + core box	water(0.5) + Al(0.5)	1.2700	102.1032	0.5000	40.1981	1	83
water refl or thermal col	water or graphite	5.4650	107.5682	2.1516	42.3497	3	86
water refl or graphite refl clad	water or Al clad	1.9050	109.4732	0.7500	43.0997	1	87
water reflector	water, water, everywhere	31.9950	141.4682	12.5965	55.6961	15	102



Table 5. Material composition (atom/b-cm) for the 2-D UMLRR HEU models.

Material	Matl ID	<sup>235</sup> U	<sup>238</sup> U	<sup>27</sup> Al	<sup>12</sup> C	<sup>16</sup> O	<sup>1</sup> H	<sup>10</sup> B	<sup>nat</sup> Cd	Pb**
Water Refl	1	—	—	—	—	3.343-2	6.686-2	—	—	—
Water+Core Box	2	—	—	3.013-2	—	1.672-2	3.343-2	—	—	—
Rad Basket+Air	3	—	—	1.366-2	—	2.066-2	4.133-2	—	—	—
Rad Basket+Water*	4	—	—	1.164-2	—	2.697-2	5.394-2	—	—	—
Graphite Refl	5	—	—	2.998-3	7.068-2	2.318-3	4.636-3	—	—	—
Full Fuel Center	6	1.361-4	1.011-5	2.135-2	—	2.142-2	4.284-2	—	—	—
Full Fuel Center+End	7	1.279-4	9.507-6	2.007-2	—	2.214-2	4.428-2	—	—	—
Full Fuel Side	8	—	—	3.541-2	—	1.379-2	2.758-2	—	—	—
Partial Fuel Center	9	6.804-5	5.057-6	2.150-2	—	2.142-2	4.284-2	—	—	—
Partial Fuel Center+End	10	6.396-5	4.753-6	2.021-2	—	2.214-2	4.428-2	—	—	—
Partial Fuel Side	11	—	—	3.541-2	—	1.379-2	2.758-2	—	—	—
Control Blade End	12	—	—	5.027-2	—	5.533-3	1.106-2	—	—	—
Control Blade Center	13	—	—	4.190-2	—	1.018-2	2.036-2	—	—	—
Control Blade Shroud	14	—	—	1.851-2	—	2.316-2	4.632-2	—	—	—
Control Blade Water	15	—	—	—	—	3.343-2	6.686-2	—	—	—
Control Blade Control	16	—	—	4.549-2	7.785-2	—	—	5.087-3	—	—
Core Box+Water+Clad	17	—	—	3.614-2	—	1.337-2	2.674-2	—	—	—
Lead Shield	18	—	—	—	—	—	—	—	—	3.296-2
Clad+Water	19	—	—	2.000-2	—	2.229-2	4.458-2	—	—	—
Thermal Column Liner	20	—	—	6.024-2	—	—	—	—	—	—
Thermal Column	21	—	—	—	8.023-2	—	—	—	—	—
Rad Basket Side	22	—	—	1.796-2	—	2.346-2	4.693-2	—	—	—
Basket Center (water)	23	—	—	5.151-3	—	3.057-2	6.114-2	—	—	—
Rad Basket Center (air)	24	—	—	9.247-3	—	1.779-2	3.558-2	—	—	—

\* This homogeneous material models a water-filled radiation basket. The basket with an air-filled bayonet is modeled as Matl #3. The 2-region radiation basket model uses Matls #22 - #24.

\*\* This density is the sum of the individual isotope densities comprising lead, where <sup>206</sup>Pb = 7.910-3, <sup>207</sup>Pb = 7.251-3, and <sup>208</sup>Pb = 1.780-2 atom/b-cm.

Table 6. Material description for the UMLRR 2-D XY Core L-1-1 configuration (actual portion of input file for GIP & DORT cases).

```
' Material by zone (description/identification):
' 1-4.  water refl
' 5-8.  water + core box  (0.5 water/0.5 Al)
' 9-12. rad basket with air filled bayonet
' 13-16. rad basket filled with water
' 17-20. graphite refl
' 21-24. full fuel center
' 25-28. full fuel center + end (0.5678 center/0.4322 edge)
' 29-32. full fuel side
' 33-36. partial fuel center
' 37-40. partial fuel center + end (0.5678 center/0.4322 edge)
' 41-44. partial fuel side
' 45-48. control blade end
' 49-52. control blade center
' 53-56. control blade shroud
' 57-60. control blade water
' 61-64. control blade control
' 65-68. Pb shield inside (0.4 water/0.6 Al)
' 69-72. Pb shield
' 73-76. Pb shield outside (0.667 water/0.333 Al)
' 77-80. Thermal Colm liner (1.0 Al)
' 81-84. Thermal Colm graphite (1.0 C12)
' 85-88. RadBasket side
' 89-92. RadBasket center (water filled)
' 93-96. RadBasket center (air filled bayonet)
```

### Space and Energy Flux Distributions for Core L-1-1

With a proper material by mesh description and a set of few group cross sections (described previously), the VENTURE code was used to compute keff and the power distribution for the Core L-1-1 system. With a relatively simple conversion of the resultant power density into a source density distribution for use by DORT, the same material distribution and a 47/20 group coupled neutron-gamma cross section library were used in DORT to compute the space and energy distribution of the neutron and gamma fluxes throughout the system. Summary results from these computations, with focus on the radiation basket regions, are given in this section.

The scalar flux distribution from DORT is read by a post-processing code (called PROCESS) and any number of first dimension, second dimension, and zone-averaged energy dependent profiles can be tabulated in a form for visualization with some auxiliary Matlab plotting routines. Here we have examples of all three distributions.

#### *Spectral Distributions (E-profiles)*

The 67-group fluxes in the central radiation basket zone in location E2 (Zone 62 in the model) were averaged over space and separated into a neutron flux vector (47 groups) and a gamma flux vector (20 groups). These data are plotted versus energy in Figs. 4 and 5, giving the desired spectra in the reactor's primary irradiation location. These two plots contain the



primary results of the current study of the spectral characteristics in the UMLRR. These distributions versus energy are typical of water-cooled thermal systems and they are qualitatively similar to the profiles generated as part of the Phase I 1-D analyses. The Phase I results, however, were determined using 199 neutron groups and 42 gamma groups. Therefore, the energy resolution with the current analysis is not as good, but the spatial resolution in the 2-D model is definitely better. Note also that the profiles in Figs. 4 and 5 are associated with the radiation basket with an air-filled bayonet located in grid position E2. The results for position C2 were very similar, since the model is nearly symmetric in the Y direction along the core mid-plane.

### ***X-Direction Spatial Distributions (I-profiles)***

To illustrate the spatial distribution of the fluxes, the DORT 67-group information was also integrated over energy to give four broad-group fluxes (three neutron groups and one gamma group). These broad-group data, for a Y location that passes through the center of the radiation basket in location E2, were plotted versus the x variable in Figs. 6 and 7 (note that a linear scale is used in Fig. 6 and a log scale is specified for Fig. 7). For the neutron data given in Fig. 6, the *fast group* includes neutrons above 0.1 MeV, the *thermal group* covers energies below 0.4 eV, and the *epithermal group* includes all energies between these limits. The gamma fine group fluxes are integrated over all energies to give a single total gamma flux, and this is compared to the total neutron flux (sum of three broad groups) in Fig. 7. As before, the spatial distributions follow expected behavior (e.g. a thermal peak in the radiation basket is apparent, the more rapid decrease in the fast and epithermal fluxes relative to the thermal flux just outside the fueled regions is expected, the significant attenuation of the gamma flux in the lead shield is as designed, etc.). These results simply quantify what was already expected.

### ***Y-Direction Spatial Distributions (J-profiles)***

A similar set of spatial flux profiles was also generated versus the axial y variable. Actually, two separate sets are illustrated here: Figs. 8 and 9 give the neutron and gamma profiles along an axial line that passes through the center of the radiation baskets in locations C2 and E2, and Figs. 10 and 11 show the same information for the axial line directly through the center of the 9x7 grid arrangement. Again, everything seen here is as expected, but the relatively wild variations in the fast and thermal fluxes are definitely interesting. In Fig. 8 for example, the fast flux peak in the center is the result of a full fuel assembly in this location (see Fig. 1 for a view of the overall geometry). Likewise, the large thermal peaks on either side of center occur because of the thermalization of the fast neutrons within the radiation baskets zones. Similarly, the oscillation-like behavior shown in Fig. 10 is due to the alternating arrangement of fuel zones and moderating regions (both side plates and water-filled control channels). In the fuel regions the fast flux is high and the thermal flux is low, and just the opposite occurs in the moderating regions.

In all, Figs. 4 - 11 give a good quantitative and qualitative picture of the neutron and gamma flux profiles in the Core L-1-1 arrangement in the UMLRR. The absolute normalization for the fluxes shown here assumed an average uniform axial power profile and then a peaking factor of about 1.4 was applied (see Ref. 5 for typical axial profiles). Thus, the flux magnitudes given here represent expected values that would be appropriate near the center of the core (where most of the material samples are irradiated). There was no normalization to experimental results.

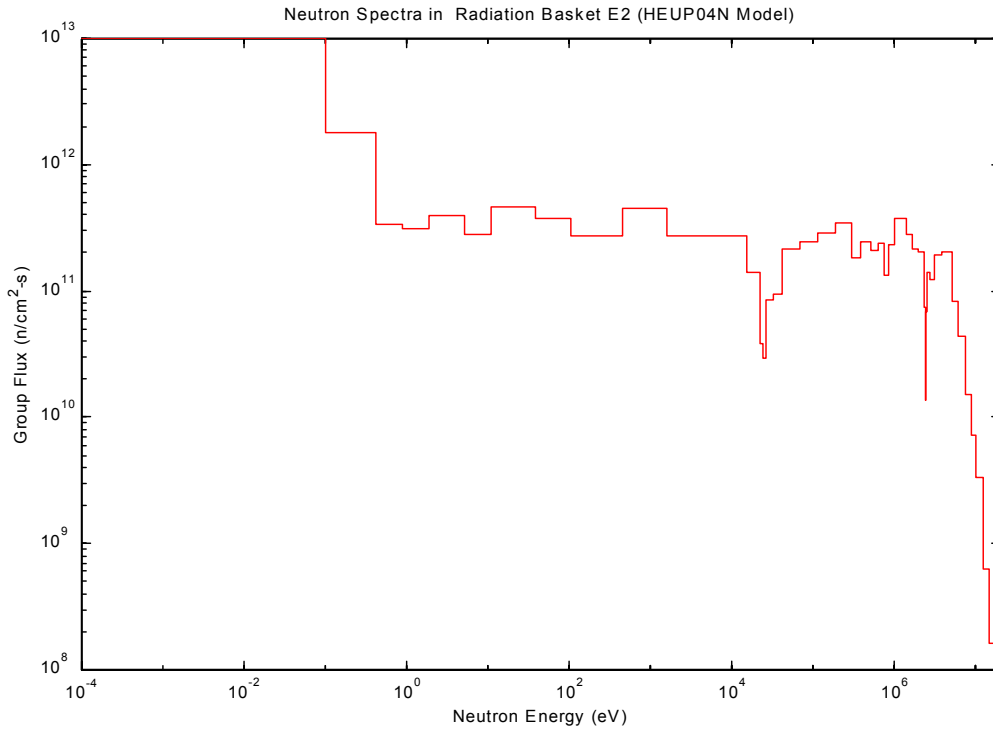


Fig. 4. Neutron flux spectrum in the radiation basket with an air-filled bayonet.

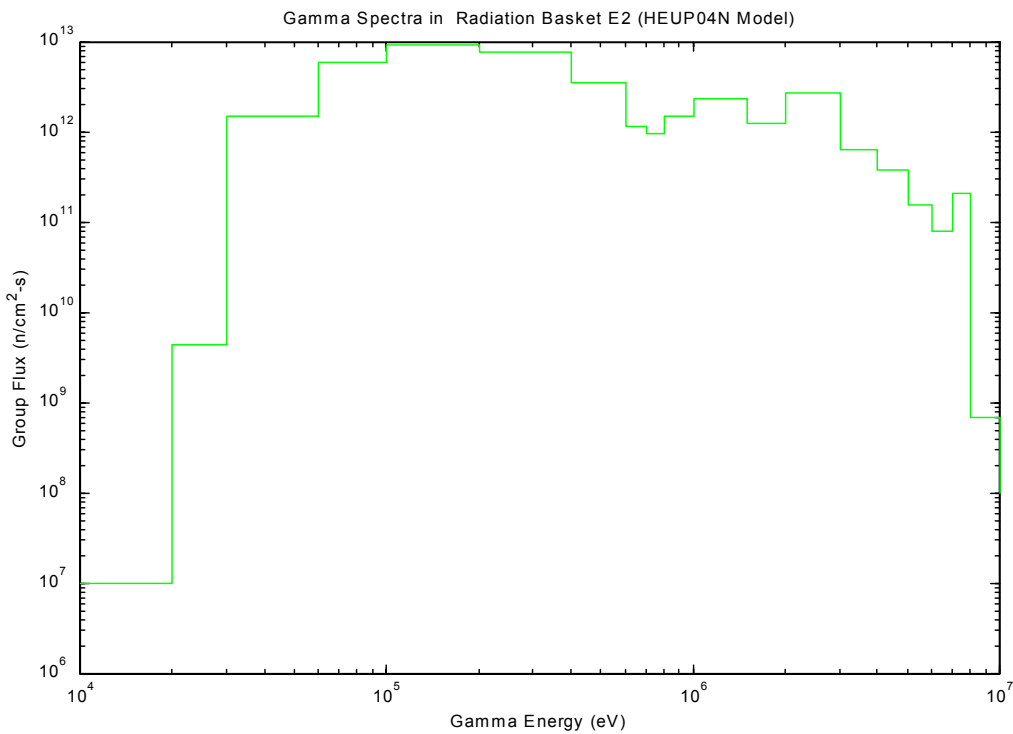


Fig. 5. Gamma flux spectrum in the radiation basket with an air-filled bayonet.

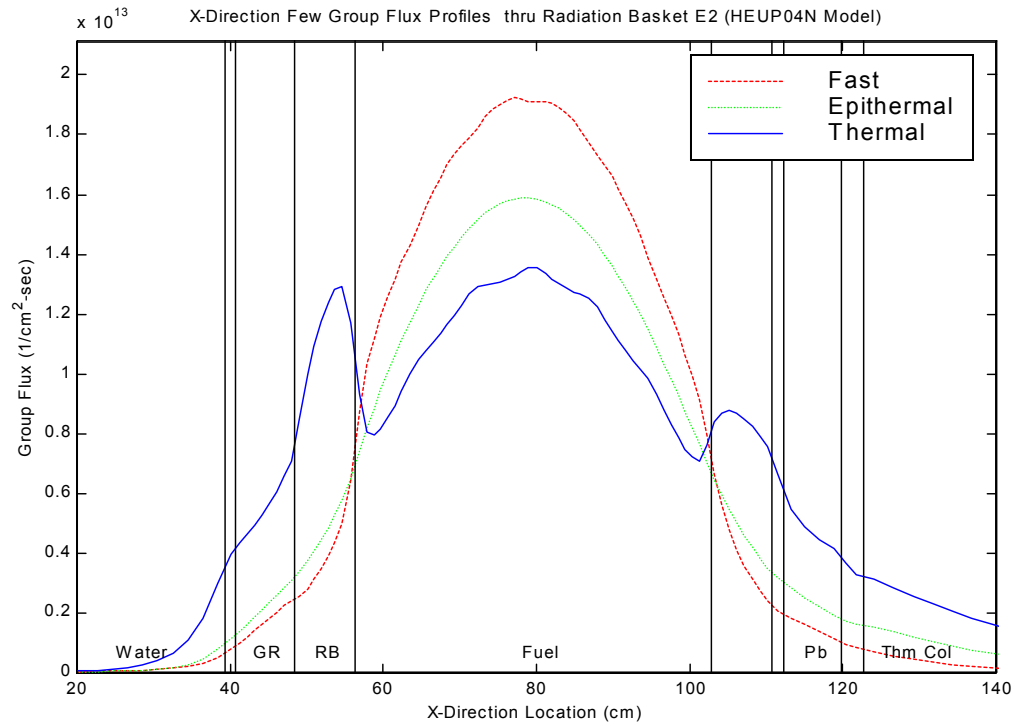


Fig. 6. X-direction broad group neutron fluxes in the UMLRR.

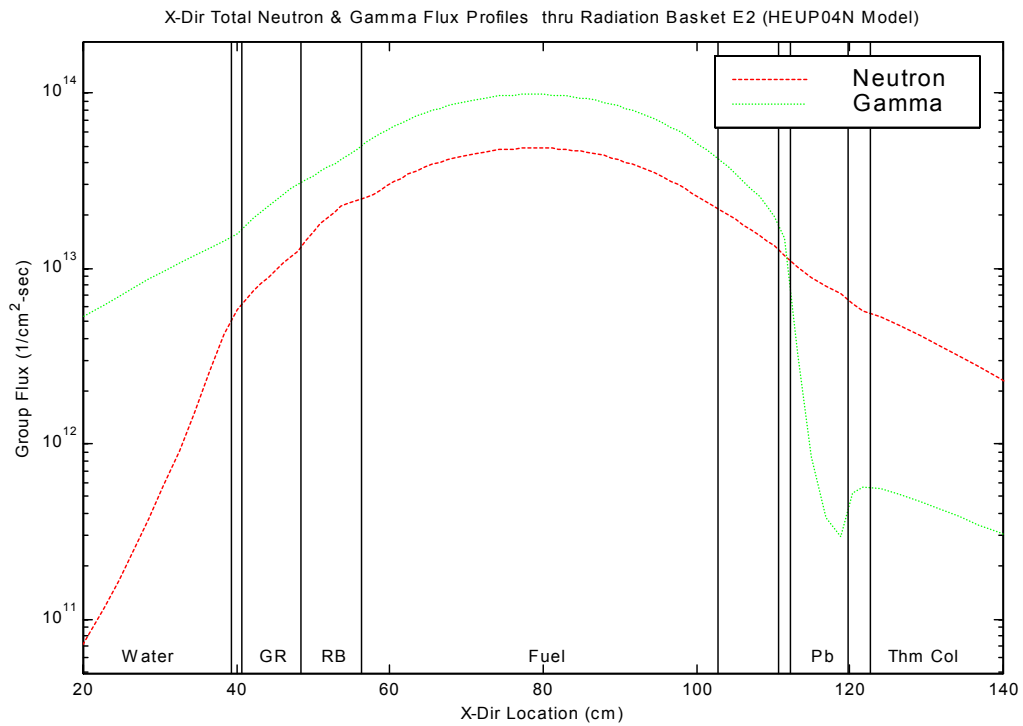


Fig. 7. X-direction total neutron and gamma fluxes in the UMLRR.

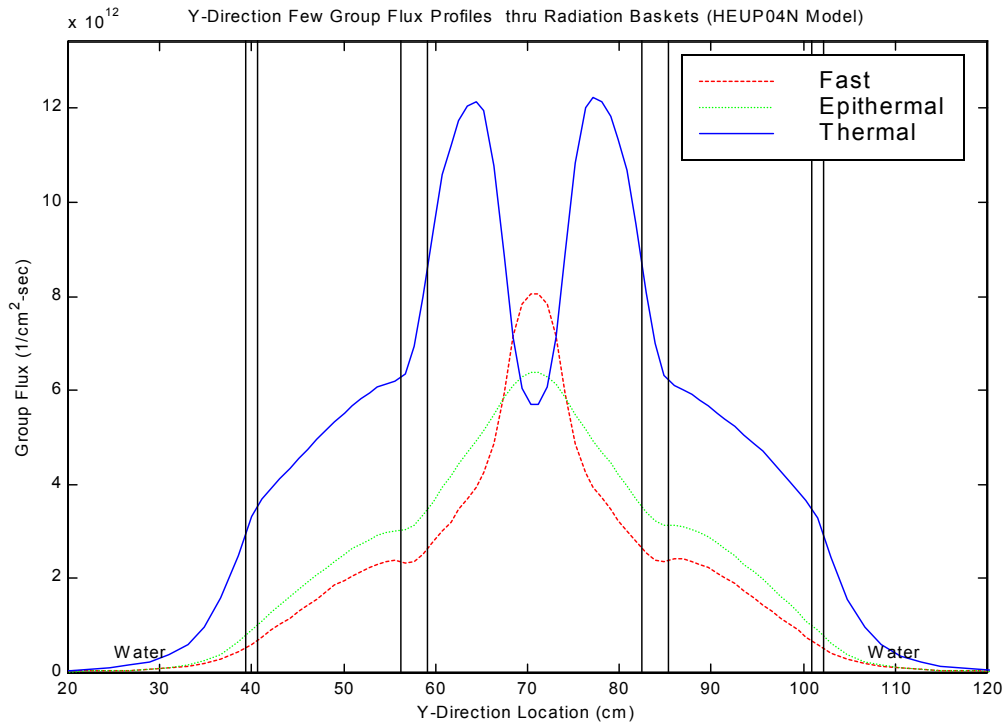


Fig. 8. Y-direction broad group neutron fluxes in the UMLRR (RadBasket).

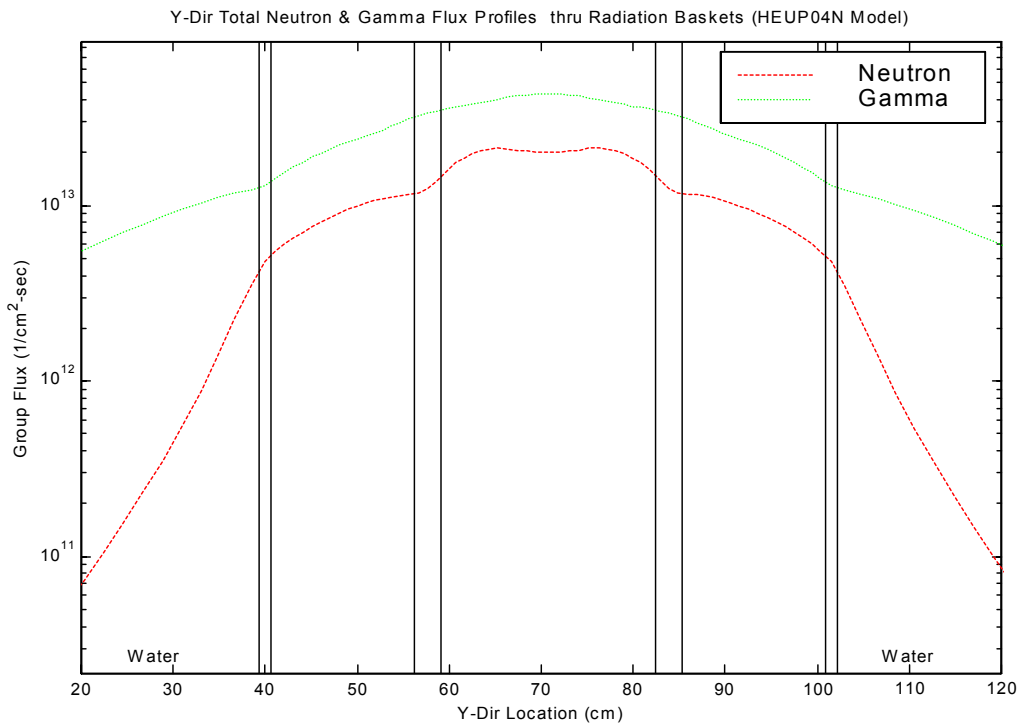


Fig. 9. Y-direction total neutron and gamma fluxes in the UMLRR (RadBasket).

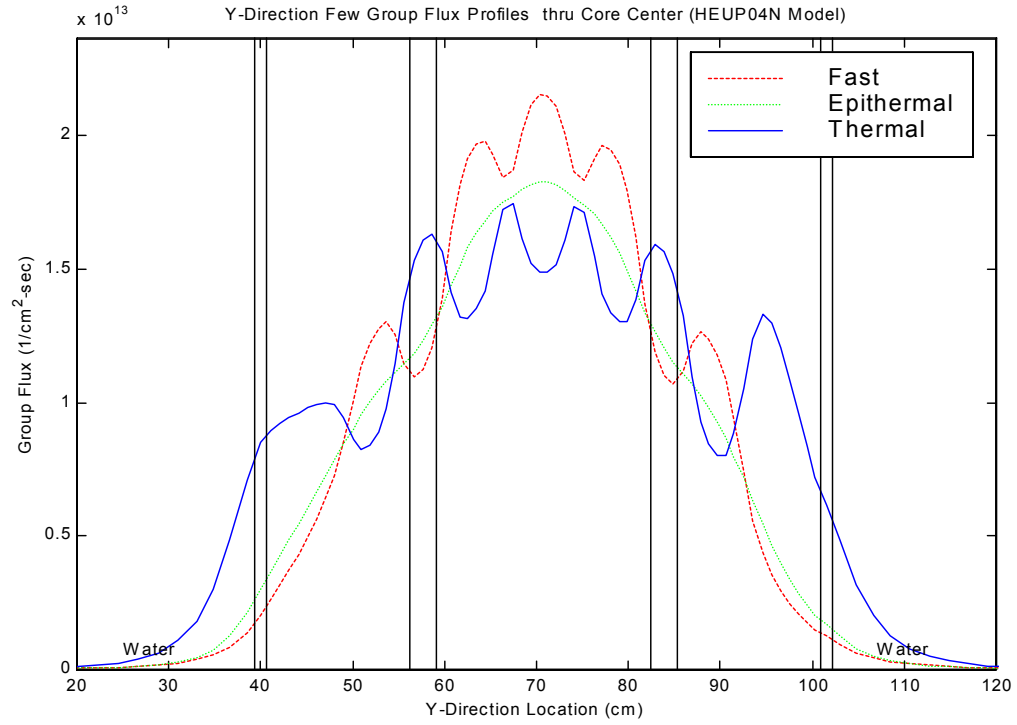


Fig. 10. Y-direction broad group neutron fluxes in the UMLRR (Core Center).

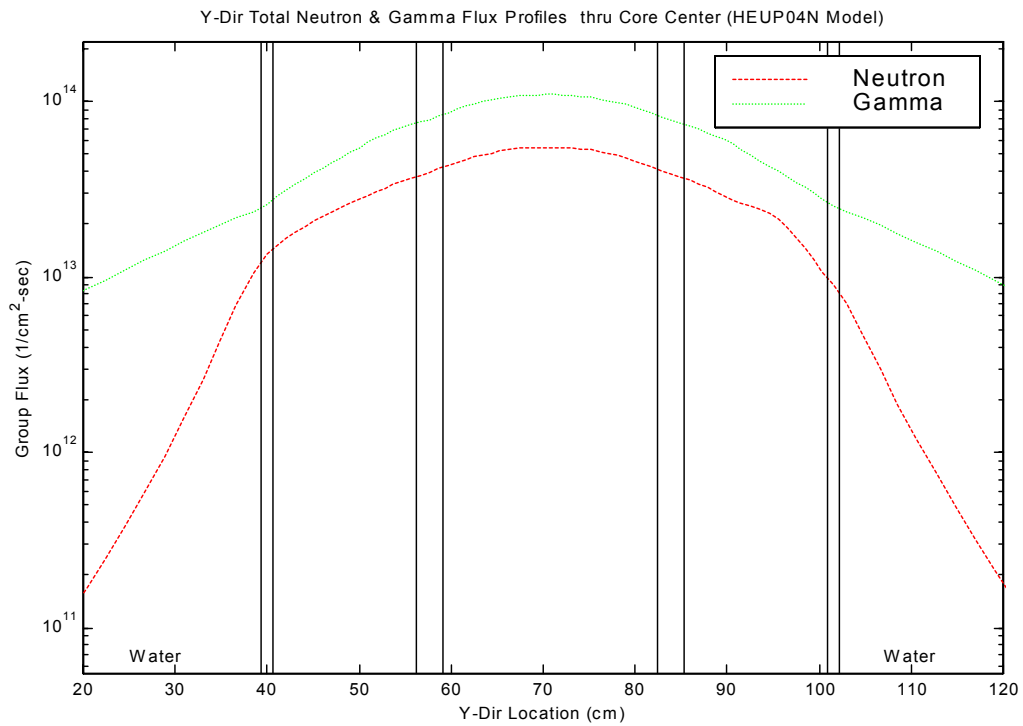


Fig. 11. Y-direction total neutron and gamma fluxes in the UMLRR (Core Center).

### Some Integral Results

One often would like to have a single number to characterize the flux spectrum in a given location and energy region. This information can be approximated from the space and energy profiles just discussed but, because the variation is so rapid in some regions, this approach is very approximate at best. However, the post-processing step mentioned above also performs integrals over energy and space as desired (defined via user input). In particular, the zone-average values of the broad-group fluxes for the central radiation basket region were extracted from the analysis and they are summarized in Table 7. A specific value for the flux above 1 MeV has also been tabulated (recall that our definition of fast flux includes all neutrons above 0.1 MeV). The greater than 1 MeV flux is frequently used in fast neutron irradiation studies to characterize the fast spectrum. In the UMLRR Core L-1-1 configuration the  $>1$  MeV flux is about  $2 \times 10^{12}$  n's/cm<sup>2</sup>-s.

Table 7. Average flux values for the radiation basket central region.

Energy Region	Average Flux (n's/cm <sup>2</sup> -s)
above 1 MeV	2.03+12
fast (> 0.1 MeV)	3.89+12
epithermal	4.81+12
thermal (< 0.4 eV)	1.17+13
total neutron	2.04+13
total gamma	3.93+13

### Summary

This report documents the general procedure used to obtain new estimates of the neutron and gamma spectra in the radiation basket regions of the UMass-Lowell Research Reactor (UMLRR). The computational model uses a relatively detailed two-dimensional representation of the actual system. The resultant neutron and gamma fluxes represent a pure computational result, since no normalizations to experimental results were made. A simple axial peaking factor was applied to give absolute fluxes that are appropriate for irradiations near the central peak in the axial profile.

This document also places some emphasis on the development of the broad-group cross sections and on the philosophy and specific approach taken in building the current model of the UMLRR. This information should be useful as base documentation for the current study and also as a basis for additional work in the future.

The flux profiles determined here give a good qualitative and quantitative indication of the spatial and spectral neutron and gamma distributions in the current Core L-1-1 configuration.

**References**

1. "BOLD VENTURE IV - A Reactor Analysis Code System, Version IV," Radiation Shielding Information Computational Center, CCC-459 (1984).
2. "DOORS3.1 - One, Two, and Three Dimensional Discrete Ordinates Neutron/Photon Transport Code System," Radiation Shielding Information Computational Center, CCC-650 (1996).
3. "SCALE 4.3 - Modular Code System for Performing Standardized Computer Analyses for Licensing Evaluation for Workstations and Personal Computers," Radiation Shielding Information Computational Center, CCC-545 (1997).
4. "VITAMIN-B6 - A Fine-Group Cross Section Library Based on ENDF/B-VI Release 3 for Radiation Transport Applications," Radiation Shielding Information Computational Center, DLC-184 (1996).
5. R. S. Freeman, "Neutronic Analysis for the Conversion of the ULR from High Enriched Uranium to Low Enriched Uranium Fuel," MS Thesis, Nuclear Engineering, University of Massachusetts Lowell (1991).